# Thermalization of Gauge Theories from their Entanglement Spectrum

Niklas Mueller,[1,2,*] Torsten V. Zache,[3,4] and Robert Ott[5]
[1]Maryland Center for Fundamental Physics and Department of Physics, University of Maryland, College Park, Maryland 20742, USA
[2]Joint Quantum Institute, NIST/University of Maryland, College Park, Maryland 20742, USA
[3]Center for Quantum Physics, University of Innsbruck, 6020 Innsbruck, Austria
[4]Institute for Quantum Optics and Quantum Information of the Austrian Academy of Sciences, 6020 Innsbruck, Austria
[5]Heidelberg University, Institut für Theoretische Physik, Philosophenweg 16, 69120 Heidelberg, Germany

(Received 18 August 2021; revised 7 February 2022; accepted 31 May 2022; published 27 June 2022)

Using dual theories embedded into a larger unphysical Hilbert space along entanglement cuts, we study the entanglement structure of $\mathbf{Z}_2$ lattice gauge theory in $(2+1)$ spacetime dimensions. We demonstrate Li and Haldane's conjecture, and show consistency of the entanglement Hamiltonian with the Bisognano-Wichmann theorem. Studying nonequilibrium dynamics after a quench, we provide an extensive description of thermalization in $\mathbf{Z}_2$ gauge theory which proceeds in a characteristic sequence: Maximization of the Schmidt rank and spreading of level repulsion at early times, self-similar evolution with scaling coefficients $\alpha = 0.8 \pm 0.2$ and $\beta = 0.0 \pm 0.1$ at intermediate times, and finally thermal saturation of the von Neumann entropy.

DOI: 10.1103/PhysRevLett.129.011601

*Introduction.*—Understanding thermalization of isolated quantum systems is an outstanding challenge in many fields, from atomic gases at ultracold temperatures [1–3], condensed matter physics [4–7], cosmology [8], to high energy and nuclear physics [9–14]. Much progress has been made in various systems based on the eigenstate thermalization hypothesis (ETH) [15–17], but not much is known for gauge theories, i.e., systems with an extensive number of local constraints.

Entanglement structure, more precisely the entanglement spectrum (ES), first suggested by Li and Haldane as an indicator of topological order (TO) in fractional quantum hall effect states [18], has recently become the subject of multiple such studies [19–27]. Their extension to lattice gauge theories (LGTs) is ambiguous because gauge invariance allows no local tensor product structure of the physical Hilbert space (HS). This issue has been addressed in recent years [28–34].

In this Letter, we use dual theories [35–37] of $\mathbf{Z}_2$ LGT in $(2+1)$ spacetime dimensions ($\mathbf{Z}_2^{2+1}$) embedded into a larger unphysical HS only along "entanglement" cuts, allowing access to the ES by naively "taking the trace." With this, we demonstrate Li and Haldane's entanglement-boundary conjecture for $\mathbf{Z}_2^{2+1}$ in the TO phase [18], analytically on an infinite half-cylinder using perturbation theory and numerically on a finite torus at arbitrary coupling. A variational approach [38] allows us to reconstruct the entanglement Hamiltonian (EH) of ground states, consistent with expectations from the Bisognano-Wichmann (BW) theorem [39,40].

Our main effort is devoted to probing thermalization of LGTs through the ES. Focusing on out-of-equilibrium dynamics after quenches with initial states in the TO, as well as the trivial (confined) phase of the model, we track the evolution of the symmetry resolved ES [41–47]: At early times the Schmidt rank is maximized, followed by the spreading of level repulsion through the ES, and saturation of the entanglement entropy at parametrically later times. Remarkably, in an intermediate stage the approach to equilibrium is characterized by self-similarity of the ES, reminiscent of classical wave turbulence and universal behavior [48–51].

Despite being restricted to small systems, our ES analysis is remarkably robust and provides a promising path towards understanding the thermalization of Abelian and non-Abelian gauge theories, e.g., in quantum chromodynamics (QCD) [14]. Our approach is suited for exploration with tensor networks [52–54] in the case of ground and low energy states, as well as near-future digital quantum computers and analog quantum simulators [55–66] (see, e.g., [67–69] for $\mathbf{Z}_2$ LGT).

*Entanglement structure of $Z_2$ gauge theory.*—We consider $\mathbf{Z}_2^{2+1}$ LGT with Hamiltonian

$$H = -\sum_{\mathbf{n}} \sigma^z_{\mathbf{n},x} \sigma^z_{\mathbf{n}+\hat{x},y} \sigma^z_{\mathbf{n}+\hat{y},x} \sigma^z_{\mathbf{n},y} - \epsilon \sum_{\mathbf{n},i=x,y} \sigma^x_{\mathbf{n},i}, \qquad (1)$$

with $\mathbf{n} = (n_x, n_y)$, $n_i \in [0, N_i - 1]$ and $i = x, y$, where $\sigma^z_{\mathbf{n},i}$ ($\sigma^x_{\mathbf{n},i}$) are Pauli operators positioned on the links of a two-dimensional rectangular lattice with $N_x \times N_y$ sites. Gauge invariance is expressed as $[H, G_{\mathbf{n}}] = 0$ with $G_{\mathbf{n}} = \sigma^x_{\mathbf{n},x} \sigma^x_{\mathbf{n}-\hat{x},x} \sigma^x_{\mathbf{n},y} \sigma^x_{\mathbf{n}-\hat{x},y}$ and Gauss law defines the physical subspace as $G_{\mathbf{n}} |\psi^{\text{phys}}\rangle = |\psi^{\text{phys}}\rangle$.

$\mathbf{Z}_2^{2+1}$ LGT has two ground state phases: a topologically trivial phase (confined), as well as a phase with topological

 

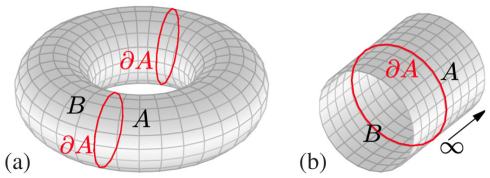


FIG. 1. Lattices with entanglement cuts considered in this work. (a) Torus and (b) infinite cylinder with entanglement boundary/boundaries $\partial A$.

order (TO). In the TO phase, for $\epsilon < \epsilon_c$, the ground state manifold is fourfold degenerate (on a torus), labeled by eigenvalues of "ribbon" operators $V_x \equiv \prod_{\mathbf{n}\in\mathcal{C}_x} \sigma^x_{\mathbf{n},i}$ and $V_y \equiv \prod_{\mathbf{n}\in\mathcal{C}_y} \sigma^x_{\mathbf{n},i}$, winding around the $x$ and $y$ directions, with $[V_x, H] = [V_y, H] = 0$ [70].

In the following, we consider the entanglement properties of a bipartition $N_x \equiv N_x^A + N_x^B$ of a torus, see Fig. 1(a). Before considering thermalization dynamics, we first validate our approach of computing LGT entanglement structure by demonstrating Li and Haldane's conjecture [18]: TO is manifest in the entanglement structure of states; the low lying part of the ES is equal (up to rescaling) to the physical spectrum of boundary excitations at the entanglement cut.

The basis of our analysis are dual formulations of Eq. (1) embedded into a larger, unphysical HS along boundaries: (a) for the torus with aforementioned entanglement bipartition [Fig. 1(a)], as well as (b) an infinite (half) cylinder with physical boundaries [Fig. 1(b)] [75]. Our dual approach is a generalization of that of Wegner [35], and unlike the latter where all Gauss laws are eliminated, it captures the entanglement structure stemming from the Gauss laws between the two subsystems, as we demonstrate below by verifying Li and Haldane's conjecture. By also resulting in a smaller Hilbert space, it reduces the numerical cost significantly compared to a direct implementation of Eq. (1).

To demonstrate Li and Haldane's conjecture, we consider first the semi-infinite cylinder A with physical "open electric" boundary conditions $\partial A$ in Fig. 1(b) [33,37]. The corresponding dual Hamiltonian reads

$$H_A = -\sum_{\mathbf{n},n_x>0} \mu^z_{\mathbf{n}} - \sum_{\mathbf{n},n_x=0} \mu^z_{\mathbf{n}}\sigma^z_{\mathbf{n},y} - \epsilon \sum_{\mathbf{n},n_x>0} \mu^x_{\mathbf{n}}\mu^x_{\mathbf{n}-\hat{x}} - \epsilon \sum_{\mathbf{n},n_x=0} \sigma^x_{\mathbf{n},y} - \epsilon \sum_{\mathbf{n},n_y>0} \mu^x_{\mathbf{n}}\mu^x_{\mathbf{n}-\hat{y}} - \epsilon \sum_{\mathbf{n},n_y=0} \mu^x_{\mathbf{n}}\mu^x_{\mathbf{n}-\hat{y}} V_y - \epsilon \sum_{n_y=1}^{N_y-1} \sigma^x_{(-1,n_y),x}. \tag{2}$$

This contains two sets of Pauli operators: dual gauge invariant operators $\mu^{x/z}_{\mathbf{n}}$ in the bulk as well as the original gauge-variant variables $\sigma^{x/z}_{\mathbf{n},i}$ on $\partial A$. Here, $\sigma^x_{(-1,n_y),x}$ is the electric flux through the boundary [75]. While gauge redundancy is eliminated in the bulk, Gauss law on $\partial A$ is not eliminated, $G_{n_y} \equiv \sigma^x_{(-1,n_y),x}\sigma^x_{(0,n_y),y}\sigma^x_{(0,n_y-1),y}\mu^x_{\mathbf{n}}\mu^x_{\mathbf{n}-\hat{y}}$ (for $n_y > 0$) and $\sigma^x_{(-1,n_y),x}\sigma^x_{(0,n_y),y}\sigma^x_{(0,n_y-1),y}\mu^x_{\mathbf{n}}\mu^x_{\mathbf{n}-\hat{y}}V_y$ (for $n_y = 0$).

To demonstrate Li and Haldane's conjecture, we first compute the boundary theory. The ground state for $\epsilon = 0$, $V_y = 1$ is given by $|\Omega^A\rangle = P_G|\uparrow\rangle$ where $|\uparrow\rangle$ is the state with plaquette eigenvalue 1, i.e., $\mu^z_{\mathbf{n}}|\uparrow\rangle = |\uparrow\rangle$ in the bulk ($n_x > 0$) and $\mu^z_{\mathbf{n}}\sigma^z_{\mathbf{n},y}|\uparrow\rangle = |\uparrow\rangle$ on $\partial A$ ($n_x = 0$); $P_G \equiv \prod_{n_y}(1 + G_{n_y})/2$ is a projector onto the physical subspace. We compute the ground state for small $\epsilon$ perturbatively [78] (see Refs. [34,79–81] for the opposite limit), resulting in a low energy effective Hamiltonian $H_A^{\text{eff}}$ describing excitations on $\partial A$ [75],

$$H_A^{\text{eff}} = -\epsilon \sum_{n_y=0}^{N_y-1} \sigma^x_{(0,n_y),y}\sigma^x_{(0,n_y-1),y}\mu^x_{\mathbf{n}}\mu^x_{\mathbf{n}-\hat{y}} + O(\epsilon^2). \tag{3}$$

Here, we omitted the projector onto $|\uparrow\rangle$, given by $\prod_{\mathbf{n}}(1 + W_{\mathbf{n}})/2$ with $W_{\mathbf{n}} = \mu^z_{\mathbf{n}}\sigma^z_{(0,n_y),y}$ ($n_x = 0$) and $W_{\mathbf{n}} = \mu^z_{\mathbf{n}}$ ($n_x > 0$), and constant terms.

We now compute the ES for $\partial A$ a (virtual) entanglement cut of the infinite cylinder $A + B$, see Fig. 1(b). The density matrix of the ground state is [at $O(\epsilon)$]

$$\rho_{A+B} = \left(\frac{1}{2} - \frac{\epsilon}{4}\left[\sum_{\substack{\mathbf{n},i \\ \notin\partial A}} \mu^x_{\mathbf{n}}\mu^x_{\mathbf{n}-\hat{i}} + \sum_{n_y=0}^{N_y-1} \sigma^x_{(0,n_y),y}\right]\right)\rho^{(0)} + \text{H.c.}, \tag{4}$$

with $\rho^{(0)} \equiv \prod_{n_y}(1 + G_{n_y})/2 \prod_{\mathbf{n}}(1 + W_{\mathbf{n}})/2$, where $W_{\mathbf{n}} = \mu^z_{\mathbf{n}}\sigma^z_{(0,n_y),y}$ for $n_x \in \{0, -1\}$ and $W_{\mathbf{n}} = \mu^z_{\mathbf{n}}$ for $n_x < -1$ and $n_x > 0$. In Eq. (4), $\mathbf{n}, i \notin \partial A$ indicates summation over links in $A + B$ away from the entanglement cut. The reduced density matrix of system $A$ follows as

$$\rho_A = \left(\frac{1}{2} - \frac{\epsilon}{4}\left[\sum_{\substack{\mathbf{n},i\in A \\ \notin\partial A}} \mu^x_{\mathbf{n}}\mu^x_{\mathbf{n}-\hat{i}} + \sum_{n_y=0}^{N_y-1} \sigma^x_{(0,n_y),y} - \sum_{n_y=0}^{N_y-1} \mu^x_{(0,n_y)}\mu^x_{(0,n_y-1)}\sigma^x_{(0,n_y),y}\sigma^x_{(0,n_y-1),y}\right]\right)\rho_A^{(0)} + \text{H.c.}, \tag{5}$$

with $\rho_A^{(0)} \equiv \mathbb{I}^{\partial A}/2^{N_y} \prod_{\mathbf{n}\in A}(1 + W_{\mathbf{n}})/2$ and $\mathbb{I}^{\partial A}$ a $2^{N_y}$ dimensional unit matrix on $\partial A$. We thus obtain the EH $H_A^{\text{ent}} = -\log(\rho_A)$ from Eq. (5),

$$H_A^{\text{ent}} = N_y \log(2) + \frac{\epsilon}{2}\sum_{n_y=0}^{N_y-1} \sigma^x_{(0,n_y),y}\sigma^x_{(0,n_y-1),y}\mu^x_{\mathbf{n}}\mu^x_{\mathbf{n}-\hat{y}}, \tag{6}$$

omitting again the projector $\prod_{\mathbf{n}\in A}(1 + W_{\mathbf{n}})/2$. Equation (6) has precisely the same form as Eq. (3),

$H_A^{\rm ent} \simeq H_A^{\rm eff}$, demonstrating (perturbatively) Li and Haldane's conjecture for $\mathbf{Z}_2^{2+1}$ lattice gauge theory.

To probe the validity of this equivalence beyond perturbation theory, we turn to numerical simulations with exact diagonalization [82]. We consider a torus separated by two entanglement cuts into systems $A+B$, shown in Fig. 1(a). The ES $\xi_n$ of states $n=1,\ldots,\dim(\rho_A)$ in $A$ is shown in Fig. 2(a), separated into symmetry sectors, specified by the electric flux operators into the system on both boundaries $(\uparrow/\downarrow)$ and a string of electric field operators $\tilde{V}_x = \prod_{\mathbf{n}\in\tilde{\mathcal{C}}} \sigma^x_{\mathbf{n},i}$ across a path $\tilde{\mathcal{C}}$ from one boundary to the other $(\pm)$ [75]. Figure 2(b) shows the smallest eigenvalues ("low energy part") of the ES compared to the boundary spectrum of $H_A$ for $\epsilon = 0.1$, displaying near perfect agreement with each other and with our perturbative result. This agreement holds in the TO phase with good precision up to finite size corrections.

Another signature of TO are entanglement gaps of the ES $\Delta_{\xi,i}$ shown in Figs. 2(a) and 2(c), the latter displaying $\Delta_{\xi,1}$ as a function of $\epsilon$. Defining the TO or confinement phase transition $\epsilon_c$ at $\Delta_{\xi,1} \to 0$ results in $\epsilon_c = 0.38 \pm 0.09$ agreeing within error bars with the infinite volume result $\epsilon_c = 0.33 \pm 0.01$ [83], see Supplemental Material [75] where we demonstrate robustness against finite-volume effects.

The Bisognano-Wichmann (BW) theorem, and its extensions [39,40], captures another aspect of the EH; it states that the EH of the ground state is a local deformation of the system Hamiltonian. Using an ansatz to approximate the reduced density matrix $\rho_A \approx \sigma_A \propto \exp\left(-\sum_{\mathbf{n}\in A} \beta_{\mathbf{n}} h_{\mathbf{n}}\right)$, with $h_{\mathbf{n}}$ denoting gauge-invariant local operators in $A$, we test its applicability to LGTs. Optimal local parameters $\beta_{\mathbf{n}}$, obtained by minimizing the relative entropy $S(\rho_A \| \sigma_A)$, are shown in Fig. 3(a) [75].

Our results are consistent with a parabolic deformation in the vicinity of the phase transition, as expected from BW for a conformal field theory. While the deformation deviates from a parabola away from the critical point, the overall quality of the approximation $H_A^{\rm ent} \approx -\log \sigma_A$ is excellent, see Figs. 3(b) and 3(c), comparing the exact ES to its variational approximation. The local deformation captures the low energy part of the ES almost perfectly for all $\epsilon$, except for small deviations at high energy which do not contribute significantly to the entanglement entropy.

*Thermalization from the entanglement spectrum.*—To characterize thermalization dynamics, we extract the ES of nonequilibrium states in the following. We prepare a (randomly chosen) excited eigenstate of $H(\epsilon = 0.1)$ as initial state and evolve with $H(\epsilon = 1)$. Figure 4(a) demonstrates thermalization, showing the corresponding Schmidt spectrum $P(n,t) \equiv \exp\{-\xi_n(t)\}$ of subsystem $A$ $[N_x \times N_y = (3+5)\times 3]$ approaching the thermal limit

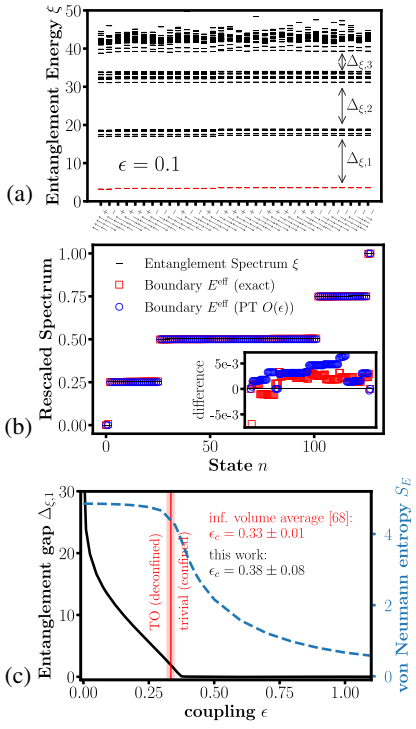


FIG. 2. (a) Entanglement spectrum $\xi_n$ of the ground state for $\epsilon = 0.1$ and $(N_x^A + N_x^B) \times N_y = (3+3)\times 3$, corresponding to the entanglement cut in Fig. 1(a), resolved into symmetry sectors. (b) Rescaled low energy part of the entanglement spectrum for $\epsilon = 0.1$, and $(N_x^A + N_x^B) \times N_y = (3+3)\times 4$, versus the spectrum of $H_A^{\rm eff}$: numerical (exact diagonalization) and analytical (perturbation theory). (c) Entanglement gap $\Delta_{\xi,1}$ between low and high energy parts of ES (black), and von Neumann entropy (blue) as a function of coupling $\epsilon$ for $(N_x^A + N_x^B) \times N_y = (3+3)\times 4$ versus infinite volume average $\epsilon_c$ from table II of [83].

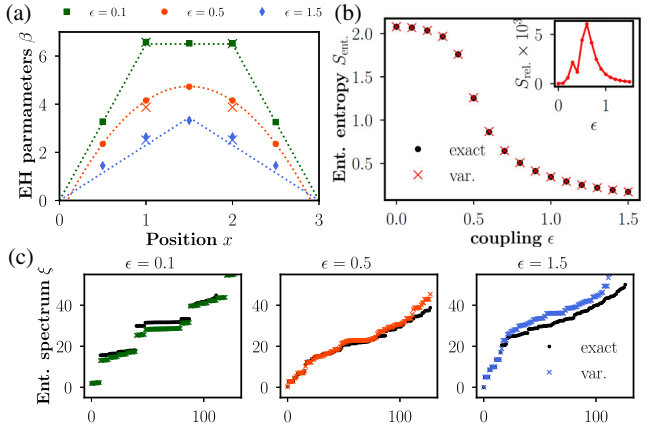


FIG. 3. (a) Optimal EH parameters for the local approximation $\sigma_A$. Thick markers and light crosses correspond to electric and magnetic energy contributions, respectively. The dotted, orange line is a parabolic fit; the other dotted, green and blue lines are guides for the eye. (b) Exact (black dots) and optimal variational (red crosses) entanglement entropy. Inset: relative entropy. (c) Exact (black dots) and optimal variational (colored crosses) ES for the same values of $\epsilon$ shown in (a). All data are obtained for a (sub)system of size $(N_x^A + N_x^B) \times N_y = (3+3)\times 2$.

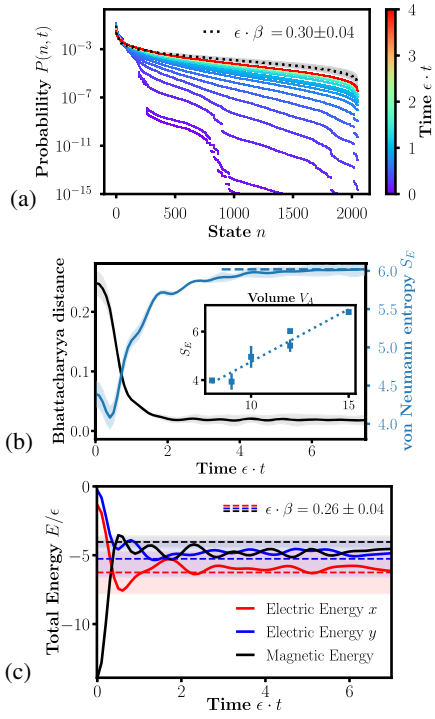


FIG. 4. (a) ES as a function of time $[(N_x^A + N_x^B)\times N_y = (3+5)\times 3]$ versus that of a thermal system (black dotted line). (b) Von Neumann entropy and Bhattacharyya distance to a thermal system. Inset: Dependence of the saturated entropy on the volume $V_A$ of $A$. (c) Electric and magnetic energy compared to thermal expectation values $(N_x \times Ny = (3+3)\times 3)$. In (a) $\beta$ is determined from the saturated entanglement entropy in (b), while in (c) it is determined from the energy density of the initial state. Bands and error bars indicate uncertainties due to finite-size effects, determined from the difference between the largest and second-largest lattices.

(black dotted line) at late times. Thermalization occurs when expectation values are equal to those derived from a canonical ensemble, i.e., $\rho_A^{\text{therm.}} = \text{Tr}_B(\rho^{\text{can.}})/\text{Tr}(\rho^{\text{can.}})$ where $\rho^{\text{can.}} = \exp\{-\beta H\}$ [84]. In Fig. 4(a), we use an approximate, but numerically simpler, form $\rho_A^{\text{therm.}} \approx e^{-\beta H_A}/\text{Tr}_A(e^{-\beta H_A})$ [84], with $H_A$ the projection of the Hamiltonian onto subsystem $A$ [boundaries are as in Eq. (2)]. In Fig. 4(b), we show the Bhattacharyya distance [85] between $\rho_A$ and $\rho_A^{\text{therm.}}$ and the von Neumann entropy, whose saturated value exhibits a volume law as displayed in the inset.

The dynamics of electric and magnetic energies is shown in Fig. 4(c) and compared with their thermal expectations, for system size $N_x \times N_y = (3+3)\times 3$. Here, $\rho_A^{\text{therm.}}$ is determined from the exact $\rho^{\text{can.}}$. To estimate the systematic error resulting from the approximate form of $\rho_A^{\text{therm.}}$ and finite volume effects, in (c) the inverse temperature $\beta \approx 0.26$ is determined by the total energy, while in (a) and (b) $\beta \approx 0.3$ it is determined from matching the saturated entanglement entropy to the thermal entropy of the same system $H_A$.

The ES allows us to characterize the stages of the thermalization process. To show this, we consider the distribution $\mathcal{P}(s_n, t)$ of level spacings $s_n = \tilde{\xi}_n - \tilde{\xi}_{n-1}$ of the unfolded ES $\tilde{\xi}_n$ [75,76], again resolved into symmetry sectors. Additionally, we consider the gap ratio [6]

$$r_n \equiv \frac{\min(\delta_n, \delta_{n-1})}{\max(\delta_n, \delta_{n-1})}, \tag{7}$$

where $\delta_n = \xi_n - \xi_{n-1} \geq 0$ of the ES $\xi_n$. Figure 5(a) shows the level spacing distribution $\mathcal{P}(s_n, t)$ at $t = 0$ (gray) and for $\epsilon\cdot t \geq 1$ (black), combined for all symmetry sectors. We compare this with a completely uncorrelated Poisson distribution (blue dotted), a Gaussian orthogonal ensemble (GOE, red dashed) and a Gaussian unitary ensemble (GUE, green dotted). Along with the distribution of the gap ratio $\mathcal{P}(r_n, t)$ in Fig. 5(b), level statistics consistent with GUE is observed for $\epsilon\cdot t \gtrapprox 0.5$ in Fig. 5(c) (black curve), well before the thermalization timescale $\epsilon\cdot t^{\text{therm.}} \approx 4$ seen in Fig. 4(b).

In order to probe the independence of thermalization on the special initial state, with large entanglement and ES level repulsion, we now consider a different scenario starting from an entirely unentangled initial state: a randomly chosen excited state of the $\epsilon \to \infty$ "electric ground state" (the confined phase). Orange curves in Figs. 5(a)–5(c) show the resulting level spacing and gap ratio approaching GUE at $\epsilon\cdot t \gtrapprox 1$ starting from the trivial

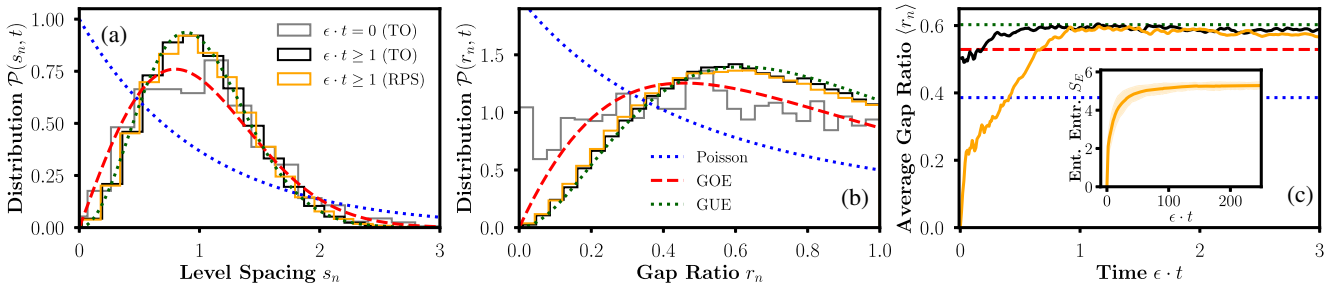


FIG. 5. (a) Distribution $\mathcal{P}(s_n)$ of level spacings (of the unfolded ES), for the quench from $\epsilon = 0.1 \to 1$ (gray and black curves) versus $\epsilon \to \infty$ (confined phase) as initial condition (orange curve). (b) Gap ratio distribution $\mathcal{P}(r_n)$. (c) Average gap ratio $\langle r_n\rangle$ as a function of time. Inset: Growth of von Neumann entropy for the quench $\epsilon = \infty \to 1$. [Shown for $(N_x^A + N_x^B)\times(3+5)\times 3$ lattice sites].

ES at $\epsilon \cdot t = 0$. The average gap ratio in (c) quickly jumps to $\langle r_n \rangle \approx 0.2$ at earliest times, then grows linearly until it saturates to about $\langle r_n \rangle \approx 0.6$. The inset of (c) shows that the growth of entanglement is much slower and saturates at parametrically later times $\epsilon \cdot t_{\text{therm.}} \lessapprox 150$, similar to the separation observed in [41] (see also [86]).

Remarkably, we find that the stage between the buildup of level repulsion and entanglement saturation is characterized by a self-similar scaling form of the spectrum $P(n,t)$, shown in Fig. 6, reminiscent of classical wave turbulence [48–51]. In this regime, the spectrum can be rescaled as $P(n,t) = \tau^{-\alpha} P(\tau^{\beta} n)$ with $\tau \equiv \epsilon(t - t_0)$. We numerically determined $\epsilon \cdot t_0 = 1.8 \pm 0.5$ and the scaling coefficients [75]

$$\alpha = 0.8 \pm 0.2 \qquad \beta = 0.0 \pm 0.1.$$

Our observation implies that thermalization occurs through turbulent transport of probability from the "high energy" (small probability) towards the low lying part of the ES (large probability). The errors quoted for $\alpha, \beta$ include finite-volume and errors from the statistical procedure of extracting them; a detailed analysis, including results on larger lattices, can be found in Supplemental Material [75].

*Summary and conclusions.*—In this Letter, we explored the entanglement structure of LGTs to characterize ground states, quantum phase transitions, and thermalization, using dual theories of $\mathbf{Z}_2^{2+1}$ embedded into a larger gauge-variant HS only along entanglement boundaries [28–31,33,34]. Our fairly simple [75] approach can be generalized to $\mathbf{Z}_n$ and $U(1)$ LGTs; non-Abelian theories [87–91] are more challenging. Ising-like dualities [87,92,93], prepotential- [94–97] and "Loop-String-Hadron" [98] formulations are promising approaches, and will be explored in future work.

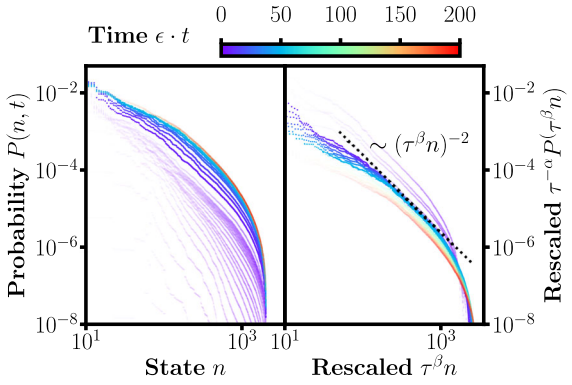


FIG. 6. Left: Unrescaled Schmidt spectrum $P(n,t) = \exp\{-\xi_n\}$ for the quench $\epsilon = \infty \to 1$ at different times. Right: Rescaled spectrum. The approach to thermalization is characterized by a self-similar universal form $P(n,t) = \tau^{-\alpha} P(\tau^{\beta} n)$, $\tau \equiv \epsilon(t - t_0)$ for times $2 \lessapprox \epsilon \cdot t \lessapprox 60 - 100$. A black dotted line indicates power law behavior $(\tau^{\beta} n)^{-2}$. The spectrum outside the scaling window is shaded out. [Shown for $(N_x^A + N_x^B) \times (3+5) \times 3$ lattice sites].

We demonstrated Li and Haldane's entanglement-boundary conjecture [18] for $\mathbf{Z}_2^{2+1}$ gauge theory, both analytically (in perturbation theory) and numerically using exact diagonalization. Moreover, we reconstructed the entanglement Hamiltonians of ground states, finding consistency with expectations from the Bisognano-Wichmann theorem [38–40] at arbitrary coupling. Using the closing of the entanglement gap of the ES, we determine the confinement or deconfinement phase transition at $\epsilon_c = 0.38 \pm 0.09$. We find agreement within error bars with the infinite volume results, demonstrating the potential usefulness of entanglement structure, compared to computing volume versus boundary law scaling of Wilson loop operators.

Our most important result is that $\mathbf{Z}_2^{2+1}$ thermalization occurs in clearly separated stages: Starting from an initial (unentangled) product state, the system maximizes its Schmidt rank quickly, followed by rapid spreading of level repulsion throughout the ES at early times. An intermediate regime is characterized by self-similar scaling of the Schmidt spectrum, reminiscent of wave turbulence and universality in (semi-)classical systems, with scaling coefficients $\alpha = 0.8 \pm 0.2$, $\beta = 0.0 \pm 0.1$.

This observation strongly hints at a reconciliation of the (naively different) quantum versus classical thermalization paradigms, i.e., in terms of matrix elements of observables [15,16] versus ergodicity, chaos and universality [48]. Because time evolution in quantum mechanics is linear, quantum chaos is hidden in the complexities of energy eigenfunctions [16], however, (and perhaps not so surprisingly [84]) it becomes evident in the entanglement spectrum. Our analysis provides a systematic path for the quantification and classification of this behavior, which is likely generic for gauge and nongauge systems and in line with the ETH. Our numerical investigations are not exhaustive, and could be extended to, e.g., studying the build-up of volume law entanglement, spectral form factors [42,76], or higher order level spacing ratios [99] of the ES. It would also be interesting to apply our techniques to systems with many-body localization [100].

Apart from the importance of $(2+1)$d LGTs for, e.g., topological quantum computation [71,101], and condensed matter physics [102,103], the entanglement structure of Abelian and non-Abelian gauge theories, such as QCD, may be crucial for thermalization in high energy and nuclear physics, where it is largely unexplored. Examples are the apparent quick thermalization and hydrodynamization of the Quark-Gluon-Plasma in ultrarelativistic heavy ion collisions [14] or the structure of QCD bound states in deeply inelastic scattering experiments [104–106].

Understanding thermalization of quantum many-body systems, in particular of gauge theories, is a unique opportunity for quantum computers and analog simulators [55–69]. Entanglement structure of quantum many-body states can be extracted in state-of-the-art quantum simulation experiments, see, e.g., [38,107–109].

N. M. thanks Zohreh Davoudi and Nikhil Karthik for valuable discussions. N. M. acknowledges funding by the U.S. Department of Energys Office of Science, Office of Advanced Scientific Computing Research, Accelerated Research in Quantum Computing program Award No. DE-SC0020312. N. M. also acknowledges support by the U.S. Department of Energy, Office of Science, Office of Nuclear Physics, under Contract No. DE-SC0012704 and by the Deutsche Forschungsgemeinschaft (DFG, German Research Foundation)—Project 404640738 during early stages of this work. R. O. acknowledges funding from the DFG (German Research Foundation) Project ID 273811115 SFB 1225 ISOQUANT'. R. O. thanks Jürgen Berges for fruitful discussions. T. V. Z. thanks Christian Kokail and Peter Zoller for valuable discussions. T. V. Z.'s work is supported by the Simons Collaboration on Ultra-Quantum Matter, which is a grant from the Simons Foundation (651440, P. Z.).

*niklasmu@umd.edu

[1] J. Eisert, M. Friesdorf, and C. Gogolin, Nat. Phys. **11**, 124 (2015).
[2] J. Schachenmayer, L. Pollet, M. Troyer, and A. J. Daley, Eur. Phys. J. Quantum Technol. **2**, 1 (2015).
[3] C. Eigen, J. A. Glidden, R. Lopes, E. A. Cornell, R. P. Smith, and Z. Hadzibabic, Nature (London) **563**, 221 (2018).
[4] R. Nandkishore and D. A. Huse, Annu. Rev. Condens. Matter Phys. **6**, 15 (2015).
[5] I. V. Gornyi, A. D. Mirlin, and D. G. Polyakov, Phys. Rev. Lett. **95**, 206603 (2005).
[6] V. Oganesyan and D. A. Huse, Phys. Rev. B **75**, 155111 (2007).
[7] F. Borgonovi, F. M. Izrailev, L. F. Santos, and V. G. Zelevinsky, Phys. Rep. **626**, 1 (2016).
[8] R. Micha and I. I. Tkachev, Phys. Rev. D **70**, 043538 (2004).
[9] R. Baier, A. H. Mueller, D. Schiff, and D. T. Son, Phys. Lett. B **502**, 51 (2001).
[10] J. Berges, Nucl. Phys. **A699**, 847 (2002).
[11] A. Arrizabalaga, J. Smit, and A. Tranberg, Phys. Rev. D **72**, 025014 (2005).
[12] V. Balasubramanian, A. Bernamonti, J. de Boer, N. Copland, B. Craps, E. Keski-Vakkuri, B. Müller, A. Schäfer, M. Shigemori, and W. Staessens, Phys. Rev. D **84**, 026010 (2011).
[13] S. Grozdanov, N. Kaplis, and A. O. Starinets, J. High Energy Phys. 07 (2016) 001.
[14] J. Berges, M. P. Heller, A. Mazeliauskas, and R. Venugopalan, Rev. Mod. Phys. **93**, 035003 (2021).
[15] J. M. Deutsch, Phys. Rev. A **43**, 2046 (1991).
[16] M. Srednicki, Phys. Rev. E **50**, 888 (1994).
[17] L. D'Alessio, Y. Kafri, A. Polkovnikov, and M. Rigol, Adv. Phys. **65**, 239 (2016).
[18] H. Li and F. D. M. Haldane, Phys. Rev. Lett. **101**, 010504 (2008).
[19] J. M. Deutsch, H. Li, and A. Sharma, Phys. Rev. E **87**, 042135 (2013).
[20] Z.-C. Yang, C. Chamon, A. Hamma, and E. R. Mucciolo, Phys. Rev. Lett. **115**, 267206 (2015).
[21] V. Khemani, A. Chandran, H. Kim, and S. L. Sondhi, Phys. Rev. E **90**, 052133 (2014).
[22] S. D. Geraedts, R. Nandkishore, and N. Regnault, Phys. Rev. B **93**, 174202 (2016).
[23] C. J. Turner, A. A. Michailidis, D. A. Abanin, M. Serbyn, and Z. Papić, Nat. Phys. **14**, 745 (2018).
[24] W. Zhu, Z. Huang, Y.-C. He, and X. Wen, Phys. Rev. Lett. **124**, 100605 (2020).
[25] D. Sels and A. Polkovnikov, arXiv:2105.09348.
[26] Y. Y. Atas, E. Bogomolny, O. Giraud, and G. Roux, Phys. Rev. Lett. **110**, 084101 (2013).
[27] O. Giraud, N. Macé, E. Vernier, and F. Alet, Phys. Rev. X **12**, 011006 (2022).
[28] P. Buividovich and M. Polikarpov, Phys. Lett. B **670**, 141 (2008).
[29] H. Casini, M. Huerta, and J. A. Rosabal, Phys. Rev. D **89**, 085012 (2014).
[30] S. Aoki, T. Iritani, M. Nozaki, T. Numasawa, N. Shiba, and H. Tasaki, J. High Energy Phys. 06 (2015) 001.
[31] S. Ghosh, R. M. Soni, and S. P. Trivedi, J. High Energy Phys. 09 (2015) 001.
[32] K. Van Acoleyen, N. Bultinck, J. Haegeman, M. Marien, V. B. Scholz, and F. Verstraete, Phys. Rev. Lett. **117**, 131602 (2016).
[33] J. Lin and D. Radicevic, Nucl. Phys. **B958**, 115118 (2020).
[34] J.-W. Chen, S.-H. Dai, and J.-Y. Pang, Nucl. Phys. **B951**, 114892 (2020).
[35] F. J. Wegner, J. Math. Phys. (N.Y.) **12**, 2259 (1971).
[36] D. Horn, M. Weinstein, and S. Yankielowicz, Phys. Rev. D **19**, 3715 (1979).
[37] D. Radievic, J. High Energy Phys. 04 (2016) 001.
[38] C. Kokail, R. van Bijnen, A. Elben, B. Vermersch, and P. Zoller, Nat. Phys. **17**, 936 (2021).
[39] J. J. Bisognano and E. H. Wichmann, J. Math. Phys. (N.Y.) **16**, 985 (1975).
[40] J. J. Bisognano and E. H. Wichmann, J. Math. Phys. (N.Y.) **17**, 303 (1976).
[41] T. Rakovszky, S. Gopalakrishnan, S. A. Parameswaran, and F. Pollmann, Phys. Rev. B **100**, 125115 (2019).
[42] P.-Y. Chang, X. Chen, S. Gopalakrishnan, and J. H. Pixley, Phys. Rev. Lett. **123**, 190602 (2019).
[43] C. Chamon, A. Hamma, and E. R. Mucciolo, Phys. Rev. Lett. **112**, 240501 (2014).
[44] Z.-C. Yang, K. Meichanetzidis, S. Kourtis, and C. Chamon, Phys. Rev. B **99**, 045132 (2019).
[45] M. Serbyn, A. A. Michailidis, D. A. Abanin, and Z. Papić, Phys. Rev. Lett. **117**, 160601 (2016).
[46] M. Mierzejewski, T. Prosen, D. Crivelli, and P. Prelovšek, Phys. Rev. Lett. **110**, 200602 (2013).
[47] B. Bertini, P. Kos, and T. Prosen, Phys. Rev. X **9**, 021033 (2019).
[48] S. Nazarenko, *Wave Turbulence* (Springer Science & Business Media, Berlin/Heidelberg, Germany, 2011), Vol. 825.
[49] J. Berges, K. Boguslavski, S. Schlichting, and R. Venugopalan, Phys. Rev. D **89**, 074011 (2014).

[50] J. Berges, K. Boguslavski, S. Schlichting, and R. Venugopalan, J. High Energy Phys. 05 (2014) 1.
[51] M. Mace, N. Mueller, S. Schlichting, and S. Sharma, Phys. Rev. Lett. **124**, 191604 (2020).
[52] Y. Meurice, R. Sakai, and J. Unmuth-Yockey, Rev. Mod. Phys. **94**, 025005 (2022).
[53] M. C. Bañuls and K. Cichy, Rep. Prog. Phys. **83**, 024401 (2020).
[54] D. Robaina, M. C. Bañuls, and J. I. Cirac, Phys. Rev. Lett. **126**, 050401 (2021).
[55] D. Kielpinski, C. Monroe, and D. J. Wineland, Nature (London) **417**, 709 (2002).
[56] C. Monroe, Nature (London) **416**, 238 (2002).
[57] A. Blais, R.-S. Huang, A. Wallraff, S. M. Girvin, and R. J. Schoelkopf, Phys. Rev. A **69**, 062320 (2004).
[58] J. I. Cirac and P. Zoller, Nat. Phys. **8**, 264 (2012).
[59] P. Hauke, F. M. Cucchietti, L. Tagliacozzo, I. Deutsch, and M. Lewenstein, Rep. Prog. Phys. **75**, 082401 (2012).
[60] J. Preskill, Quantum **2**, 79 (2018).
[61] E. A. Martinez, C. A. Muschik, P. Schindler, D. Nigg, A. Erhard, M. Heyl, P. Hauke, M. Dalmonte, T. Monz, P. Zoller *et al.*, Nature (London) **534**, 516 (2016).
[62] N. Klco, E. Dumitrescu, A. McCaskey, T. Morris, R. Pooser, M. Sanz, E. Solano, P. Lougovski, and M. Savage, Phys. Rev. A **98**, 032331 (2018).
[63] T. V. Zache, F. Hebenstreit, F. Jendrzejewski, M. Oberthaler, J. Berges, and P. Hauke, Quantum Sci. Technol. **3**, 034010 (2018).
[64] Z. Davoudi, M. Hafezi, C. Monroe, G. Pagano, A. Seif, and A. Shaw, Phys. Rev. Research **2**, 023015 (2020).
[65] A. Mil, T. V. Zache, A. Hegde, A. Xia, R. P. Bhatt, M. K. Oberthaler, P. Hauke, J. Berges, and F. Jendrzejewski, Science **367**, 1128 (2020).
[66] W. A. de Jong, K. Lee, J. Mulligan, M. Płoskoń, F. Ringer, and X. Yao, arXiv:2106.08394.
[67] C. Schweizer, F. Grusdt, M. Berngruber, L. Barbiero, E. Demler, N. Goldman, I. Bloch, and M. Aidelsburger, Nat. Phys. **15**, 1168 (2019).
[68] L. Barbiero, C. Schweizer, M. Aidelsburger, E. Demler, N. Goldman, and F. Grusdt, Sci. Adv. **5**, eaav7444 (2019).
[69] L. Homeier, C. Schweizer, M. Aidelsburger, A. Fedorov, and F. Grusdt, Phys. Rev. B **104**, 085138 (2021).
[70] $V_x$, $V_y$ are electric flux loops winding around the periodic $x$- and $y$-directions of the torus, so called "ribbon" operators [71,72], see also [73,74].
[71] A. Y. Kitaev, Ann. Phys. (Amsterdam) **303**, 2 (2003).
[72] S. Sachdev, Rep. Prog. Phys. **82**, 014001 (2019).
[73] C. Michael, J. Phys. G **13**, 1001 (1987).
[74] P. van Baal and J. Koller, Ann. Phys. (N.Y.) **174**, 299 (1987).
[75] See Supplemental Material at http://link.aps.org/supplemental/10.1103/PhysRevLett.129.011601 for details of the dual formulations, entanglement Hamiltonian extraction, and additional finite volume studies, which includes [26,33,35–37,51,76,77].
[76] T. Guhr, A. Müller-Groeling, and H. A. Weidenmüller, Phys. Rep. **299**, 189 (1998).
[77] S. Kullback and R. A. Leibler, Ann. Math. Stat. **22**, 79 (1951).
[78] S. Bravyi, D. P. DiVincenzo, and D. Loss, Ann. Phys. (Amsterdam) **326**, 2793 (2011).
[79] A. Patkós and F. Deak, Z. Phys. C **9**, 359 (1981).
[80] N. H. Dass, A. Patkos, and F. Deák, Nucl. Phys. **B205**, 414 (1982).
[81] A. Patkos and N. H. Dass, Phys. Lett. **119B**, 391 (1982).
[82] P. Weinberg and M. Bukov, SciPost Phys. **7**, 020 (2019).
[83] H. W. J. Blöte and Y. Deng, Phys. Rev. E **66**, 066110 (2002).
[84] J. R. Garrison and T. Grover, Phys. Rev. X **8**, 021026 (2018).
[85] A. Bhattacharyya, Bull. Calcutta Math. Soc. **35**, 99 (1943).
[86] P. Calabrese and J. Cardy, J. Phys. A **42**, 504005 (2009).
[87] B. Douçot, L. B. Ioffe, and J. Vidal, Phys. Rev. B **69**, 214501 (2004).
[88] I. Raychowdhury and J. R. Stryker, Phys. Rev. D **101**, 114502 (2020).
[89] Z. Davoudi, I. Raychowdhury, and A. Shaw, Phys. Rev. D **104**, 074505 (2021).
[90] A. Ciavarella, N. Klco, and M. J. Savage, Phys. Rev. D **103**, 094501 (2021).
[91] U.-J. Wiese, Philos. Trans. R. Soc., A **380**, 20210068 (2021).
[92] J. Drouffe, C. Itzykson, and J. Zuber, Nucl. Phys. **B147**, 132 (1979).
[93] M. Mathur and T. P. Sreeraj, Phys. Rev. D **92**, 125018 (2015).
[94] M. Mathur, J. Phys. A **38**, 10015 (2005).
[95] M. Mathur, Nucl. Phys. **B779**, 32 (2007).
[96] R. Anishetty and I. Raychowdhury, Phys. Rev. D **90**, 114503 (2014).
[97] M. Mathur, I. Raychowdhury, and R. Anishetty, J. Math. Phys. (N.Y.) **51**, 093504 (2010).
[98] I. Raychowdhury and J. R. Stryker, Phys. Rev. Research **2**, 033039 (2020).
[99] S. H. Tekur and M. Santhanam, Phys. Rev. Research **2**, 032063(R) (2020).
[100] M. Brenes, M. Dalmonte, M. Heyl, and A. Scardicchio, Phys. Rev. Lett. **120**, 030601 (2018).
[101] K. Satzinger, Y. Liu, A. Smith, C. Knapp, M. Newman, C. Jones, Z. Chen, C. Quintana, X. Mi, A. Dunsworth *et al.*, Science **374**, 1237 (2021).
[102] V. Kasper, G. Juzeliūnas, M. Lewenstein, F. Jendrzejewski, and E. Zohar, New J. Phys. **22**, 103027 (2020).
[103] X.-G. Wen, *Quantum Field Theory of Many-Body Systems: From the Origin of Sound to an Origin of Light and Electrons* (Oxford University Press Oxford, on Demand, 2004).
[104] D. E. Kharzeev and E. M. Levin, Phys. Rev. D **95**, 114008 (2017).
[105] N. Mueller, A. Tarasov, and R. Venugopalan, Phys. Rev. D **102**, 016007 (2020).
[106] Z. Tu, D. E. Kharzeev, and T. Ullrich, Phys. Rev. Lett. **124**, 062001 (2020).
[107] H. Pichler, G. Zhu, A. Seif, P. Zoller, and M. Hafezi, Phys. Rev. X **6**, 041033 (2016).
[108] M. Dalmonte, B. Vermersch, and P. Zoller, Nat. Phys. **14**, 827 (2018).
[109] A. Elben, R. Kueng, H.-Y. R. Huang, R. van Bijnen, C. Kokail, M. Dalmonte, P. Calabrese, B. Kraus, J. Preskill, P. Zoller, and B. Vermersch, Phys. Rev. Lett. **125**, 200501 (2020).